Available online at www.sciencedirect.com

SciVerse ScienceDirect

Energy Procedia 00 (2014) 000–000

Energy Procedia

www.elsevier.com/locate/procedia

SHC 2013, International Conference on Solar Heating and Cooling for Buildings and Industry
September 23-25, 2013, Freiburg, Germany

A Novel Approach to the Analysis of Hydraulic Designs in Large Solar Collector Arrays

Philip Ohnewein[a], Robert Hausner[a]

[a]*Solar thermal components and systems, AEE – Institute for Sustainable Technologies (AEE INTEC)*
Feldgasse 19, Gleisdorf, 8200, Austria. Tel +43 3112 5886-255, fax +43 3112 5886-18, p.ohnewein@aee.at

Abstract

In the present paper, we focus on the analysis of solar collector arrays, a key technical component in large solar thermal systems. We identify two main problems: (1) For large collector arrays, there are currently no satisfactory methods for a simple and straightforward technical assessment and comparison of different hydraulic design options. In response, we developed a key figure framework that allows concise characterization and comparison of different design options for collector arrays. The characterization is based on a set of straightforward key figures that assess the main technical phenomena. All key figures may be computed in a theoretical analysis at design time, and therefore our work improves the detailed collector array design in the engineering phase. (2) We identify a gap in missing scientific input for solar thermal engineering tools: The pressure losses of T-pieces that couple absorber pipes with header pipes in a solar collector are largely unknown under the boundary conditions found in solar thermal systems. In response, we carried out an extensive experimental study measuring pressure loss values of T-pieces. Based on the (1) the key figure framework and (2) the know-how about T-pieces, the main target of our work is to increase planning reliability, to contribute to trouble-free operation of large solar thermal plants and to minimize solar thermal energy cost.

Selection and peer review by the scientific conference committee of SHC 2013 under responsibility of PSE AG.

Keywords: collector arrays; hydraulic design; system design; solar energy cost; key figures; T-pieces

1. Introduction

Large-scale solar thermal systems offer significant potentials in terms of energy yield and contribution to the overall thermal energy supply. Large-scale systems are gaining importance on the market, as solar energy cost in some cases is on the same level with conventionally generated heat [4].

Selection and peer review by the scientific conference committee of SHC 2013 under responsibility of PSE AG.

Over the last years, a considerable increase in the knowledge about large-scale solar thermal systems has taken place, with numerous contributions from both the scientific community and realized large-scale systems. Technical guidelines for large-scale systems have been released [15], and several R&D reports and text books summarize the state of knowledge [11, 12, 10, 13].

2. Problem

One of the key tasks in planning large solar thermal plants is the hydraulic design of the collector array. The authors believe that, for what concerns large collector arrays, the available technical literature does not provide sufficient detailed information, as some technical aspects essential for large systems have not been answered satisfactorily or were not taken into consideration at all. We identify three main problems:

a) There are currently no satisfactory methods for a simple and straightforward technical characterization, assessment and comparison of different hydraulic design options for large collector arrays.
b) For what concerns tools to simulate the hydraulic and thermal behavior of large collector arrays, one key issue is the poor validation by appropriate experimental measurements.
c) To some extent, the scientific basis for the validation mentioned in b) is missing. This gap concerns the T-pieces which are found in solar collectors, where small absorber pipes are joined with header pipes. There is currently a lack of reliable pressure loss data for these T-pieces. Figures or analytical models available in standard literature are mostly not useful for solar thermal applications due to several reasons which we explain in this paper.

3. Objectives and Results

How are the problems described above tackled in our work?

As to problem a), the characterization of design options for large collector arrays, the first objective of our work is to generate a set of key figures: 11 characteristic key figures provide a simple and straightforward way to assess and to compare different design options for solar collector arrays. The intention is to provide a quick overview of the main technical phenomena, allowing direct comparisons of different concepts and design options for collector array layouts. Several key figures are also relevant for considerations about solar thermal energy cost. All the presented key figures may be computed in a theoretical analysis at design time, and therefore our work improves the detailed collector array design in the engineering phase.

As to problem b), a computational tool for solar thermal plants developed and used by the authors [1] shall be validated based on systematic comparisons with specific experimental measurements. However, a solution to problem b) requires an answer to problem c): Understanding the behavior of T-pieces is crucial in order to model physical phenomena in solar collectors, most notably the pressure loss and flow distribution between absorber pipes, and as a consequence temperature distribution and total pressure drop. Since the relevant information available in scientific literature proved to be insufficient (see chapter 5 for a detailed discussion), we decided to determine the required pressure loss values in a series of experiments. To our knowledge, this is the first time that an extended experimental study on T-piece pressure losses focuses on operating conditions relevant for solar thermal systems. We covered a wide range of Reynolds numbers, geometries and volume flow ratios.

Based on the measurement results for the pressure loss of T-pieces, a systematic validation of the computational tool [1] will follow, but this is out of the scope of the present paper. The use of a simple and validated tool is important as it allows quick, yet reliable and accurate, detailed engineering work on collectors and collector arrays, without having to resort to expensive methods like CFD or FEM. The main features of the computational tool include:

- ability to theoretically calculate collector efficiencies on a very detailed level
- static simulation of collector arrays based on an accurate hydraulic-thermally coupled model
- flexibility to implement new results, such as the key figures defined in section 4 of this paper

While the nature of our work is technical, the ultimate purpose is more market-oriented: minimizing the levelized solar energy cost while maximizing operational reliability and safety over a plants' lifetime. This means that both investment and ongoing costs (maintenance and running cost such as pump electricity) are relevant, but we also put a clear focus on energy yields and technical safety of collector arrays.

Our overall target is not primarily to develop optimal collector arrays, but to provide a technical-scientific basis for the development of optimal collector array designs, in terms of both technology and economy. We would also like to stress that we are not in favor of any particular collector array design or collector type. Rather, our aim is to present a concept that is open and applicable to various collector array designs.

The structure of this paper is organized in the following way: In section 4, we discuss selected technical aspects about the design of large collector arrays, and then we start with the definition of the mentioned key figures for characterizing collector arrays. Next, we define two example collector arrays and compare them based on the set of newly-defined key figures. In section 5, we focus on the pressure loss of T-pieces: We discuss why the available information in scientific literature is insufficient, before we present a few selected results of our experimental study. We close the paper in section 6 with a review of the findings and some thoughts on the next steps in our work.

4. Characteristic Key Figures

Independently from the collector type used, large collector arrays always need to have some components connected in parallel, such as absorber pipes or collector rows. Now, one principal technical problem is the fact that parallel hydraulic connections of system components always lead to a more or less uneven flow distribution between the components [3, 7, 17]. Inhomogeneous flow distribution is the starting point of a series of technical phenomena that limit the maximum collector areas that may be connected in one array. Both U- or Z-layouts – see [5] for a definition of these terms – are affected, yet to different degrees. In practice, a certain degree of flow inequality can be tolerated. VDI [15] includes the recommendation that the mass flows of all collectors in an array should not differ by more than ±10%. While the source gives no explanation as to the choice of this value, we believe that the value of ±10% is too restrictive; section 4.3 has more details about this.

4.1. Definition of the characteristic key figures

The objective that we pursue in the development of the characteristic key figures has been described in section 3 of this paper. In the following, the current state of the key figures development is described in detail. Some other aspects of system layout (such as the integration into other processes, heat exchanger design etc.) are beyond the scope of the work presented in this paper.

Stagnation distance [K]

Uneven flow distribution in solar collector arrays results in uneven temperature distribution. Absorber pipes with the smallest mass flows reach the highest temperatures. In extreme cases, the local boiling temperature of the heat transfer fluid is exceeded and partial stagnation occurs, an effect that must be avoided.

The 'minimum stagnation distance' is defined as the temperature difference between the local boiling temperature and the hottest of all absorber pipe flow temperatures, taking into account the entire collector array. In contrast, the 'average stagnation distance' refers to the average flow temperature of the entire collector array. The comparison between the minimum and the average stagnation distance provides a straightforward way to assess the risk for partial stagnation to occur at some spot of the collector array.

One has to keep in mind that there is not one threshold value that the minimum stagnation distance should not fall below. Rather, relatively small stagnation distances may occur in normal plant operation, depending on system design, the choice of heat transfer medium, system pressure and operating conditions.

From the point of view of collector array design, as a rule one can conclude: large collector arrays, inhomogeneous flow distribution, small operating pressure and high flow temperatures all lower the minimum stagnation distance.

In case the flow temperatures are elevated, also the ratio of minimum to average stagnation distance, expressed in percent, is significant. In any case, small values are an indication of increased risk for partial stagnation.

Maximum flow velocity [m/s]

While it is not easy to set a specific threshold value for the flow velocity in a solar collector array, very high flow velocities are not permissible as they elevate the risk for erosion corrosion which could damage the pipe walls or eventually destroy them. Hence, high flow velocities have to be avoided by increasing pipe diameters or by changing the array layout. The key figure presented here is defined as the maximum flow velocity in all collector array pipes (all connecting pipes, absorber pipes and header pipes in collectors), regardless of the used pipe material.

Absorber pipe Reynolds numbers [#]

For the same design conditions, different absorber pipe Reynolds number can be attained based on the temperature levels, heat transfer fluid, solar collector design and the chosen solar array layout (hydraulic lengths). Higher absorber Reynolds numbers imply improved heat transfer in the absorber and thus increase the thermal efficiency of the system. Since flow conditions vary significantly within a collector array, this key figure is defined as the range of minimum and maximum absorber Reynolds numbers, taking into account all absorber pipes of the array.

Specific metal mass of array piping [kg_{steel}/m^2_{gr}]

Different solar array layout options require a different extent of pipe work, both in terms of pipe length and pipe diameters. Minimizing the piping effort is one way to reduce the solar energy cost. In order to encompass different design options into one value, this key figure includes the metal mass of all collector array pipes (outside the collectors) in relation to the overall gross area of all collectors in the array. Steel is assumed since it is most commonly used as piping material.

Piping network length [cm/m^2_{gr}]

The total network length of the collector piping is another measure for the overall piping effort of a collector array. For the definition of this key figure, the total network length (as opposed to the total piping length) is set in relation to the overall gross area of the collector array. This key figure differs from the previous one, the metal mass, in that it does not focus on the piping itself, but on the effort that has to be made in order to place the piping of the collector array. This is especially important in case the collector array pipework is laid underground: In this case, the piping network length.

Specific copper mass in solar collector [kg_{Cu}/m^2_{gr}]

Depending on the chosen collector array design, increasing the header pipes in the inside of solar collectors presents a way to obtain more homogeneous flow distribution and decrease pressure losses. This, however, is at the expense of the solar collector price which is strongly affected by the amount of metal used for the collector-internal piping. This key figure sums up the weight of all copper pipes in the collector, relative to the collector gross area. We chose copper since it is widely used as piping material and it is expensive. The absorber plate, often made of aluminum, is not taken into account.

Thermal capacity of the collector array [$kJ/m^2_{gr}\cdot K$]

Capacitive energy losses occur in a solar plant due to the overall thermal capacity of the collector array which needs to be heated from ambient to operating temperature levels at least once per operating day. In other words, the absolute heat capacity of all collectors, the collector array piping and the heat transfer fluid is characteristic for the start-up losses of a collector array. Pipe lengths and dimensions, the heat capacity of the collectors and the employed

heat transfer fluid must be known (see section 4.2 for an example). The heat insulation of the collector array piping is neglected, and no distinction is made between pipes exposed to air or to terrain. The key figure is expressed relative to the total array gross area.

Total collector array pressure loss [bar]

This key figure is defined as the total pressure loss of the collector array alone, at specific operating conditions. It comprises friction and minor pressure losses in the collector array, including the connecting pipes, main supply and return pipes and any hydraulic elements installed in the collector array (e.g. balancing valves). Hydraulic elements typical of the technical cabinet (e.g. heat exchanger, non-return valve etc.) are not taken into account, because they are hardly affected by the collector array design.

The significance of this key figure is associated with safety aspects. While there is not a specific maximum allowable value for the total pressure loss of the collector array, the pressure loss is limited by safety-related technical reasons such as: actual operating and maximum permissible pressure in the solar collector, stagnation distance (see above), pump pressure head, pump NPSH (Net Positive Suction Head), filling pressure of the expansion vessel, and last but not least dimensioning of the safety valve. Depending on the collector array layout, very large systems might reach a limit range.

Ratio of hydraulic to thermal power [W_{hyd} / kW_{th}]

Considering merely the absolute pressure loss of a collector array is not sufficient for comparing different layout options or for giving an estimation of the expected operating cost due to pump electricity. The effort of the pump (in terms of hydraulic power) in order to generate a defined solar thermal power output, at specific operating conditions, is a better measure of the operating cost.

Efficiency loss due to uneven flow distribution [%]

Uneven temperature distribution between the solar collectors leads to a decrease in the overall thermal efficiency of an array. This is due to the fact that collector efficiency curves decay stronger than linear: Due to this, the efficiency decrease of collectors operated at higher temperatures (smaller collector flow rates) is stronger than the increase that can be gained at lower temperatures (higher collector flow rates).

For this key figure, the theoretical thermal efficiency of a collector array with perfectly even flow distribution – but otherwise identical to the real one – is calculated. The key figure is defined as the ratio between the overall thermal efficiency of the array with the real (more or less uneven) flow distribution to the theoretical idealized thermal efficiency.

Overall emptying behavior [in words]

In terms of operating safety, stagnation presents a serious risk, especially for large collector arrays with efficient collectors and high power outputs. Collectors and collector connections behaving well in case of stagnation are one key for handling this risk, although strategies exist for handling stagnation or overheating. For this key figure, the emptying behavior of a collector and collector array is assessed in qualitative way.

4.2. Reference collector arrays: Definition

The choice of good collector array designs depends entirely on the employed collector type. The two tasks – choosing a good collector and finding a good array design – cannot be thought independently. In this section, two reference collector arrays are presented: The two are based on different collector types, and each has a total gross collector area of 4800 m². See figure 1 and table 1 for details about the collectors. For details about the reference collector arrays and the operating conditions used in the calculations, see figure 2.

One of the reference collectors is a harp type, the other one is a meander type. In the harp reference array, 16 harp collectors are connected in series to form one collector row; 20 such rows are connected in parallel. In the meander array, two groups of collectors are connected in series to form one row. In each group, 16 collectors are connected in

parallel by internal manifolding. It is possible to do so because the meander reference collector has 4 header pipe connections. In both reference collector arrays, the rows have relatively high pressure losses compared with the pressure losses in the connecting pipes. This so-called high authority of the rows is the true reason for the good hydraulic behavior in terms of flow distribution. The high absorber pipe pressure losses needed for high absorber authority within a group is achieved by a smaller absorber pipe diameter compared to the harp collectors (7.2mm vs. 9.2mm); at the same time, the header pipe dimension is larger compared to the harp collectors (39mm vs. 32mm).

The work presented in this section is not limited to harp or meander collector types and can be applied to different choices of collectors and collector arrays. Also, the authors would like to emphasize that they do not give preference to any specific collector design, be it flat-plate collectors or not. Rather, the aim is to obtain a comparison and technical assessment of different concepts. While both reference collector types are suitable for large plants, they are mere designs dummies that were developed solely for the scope of the present work; they are not intended for production and have been intentionally chosen in order to avoid overlaps with collectors available on the market as far as possible.

4.3. Reference collector arrays: Results and Discussion

We performed a detailed analysis of the reference collector arrays and calculated the key figures presented in section 4.1, using the computational toolset mentioned in the Introduction of this paper [1]. See table 1 for an overview on the assumed operating conditions in the calculations.

The collector array using the harp collector is on the left, the meander array on the right. Overall size, row

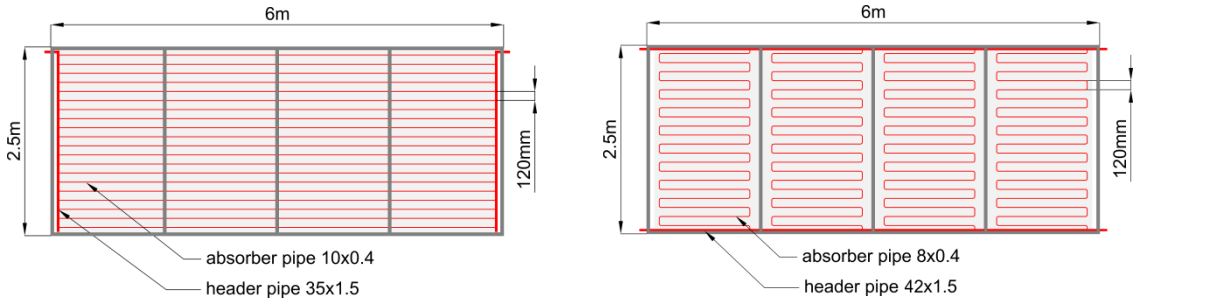

Figure 1: Harp and meander collectors used in the reference collector arrays

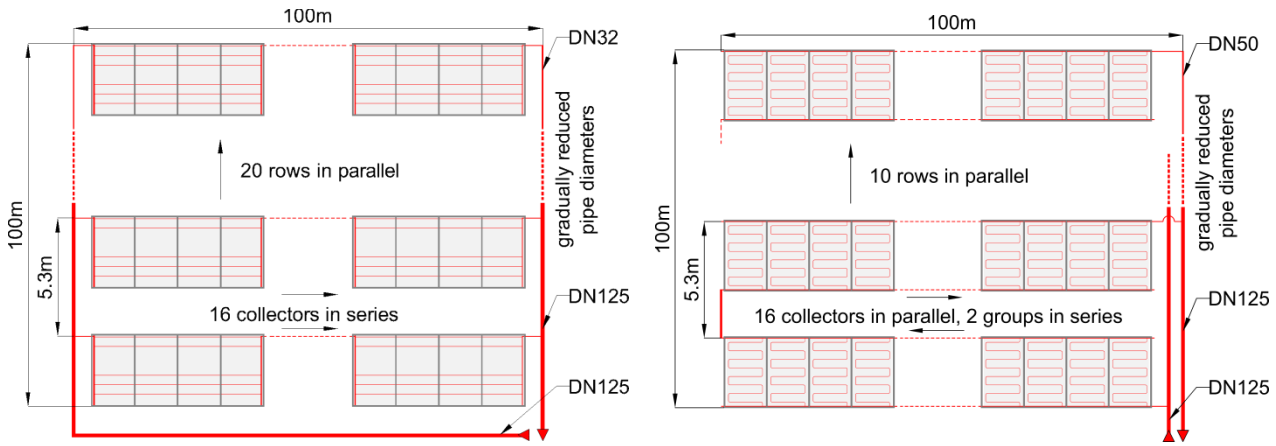

Figure 2: General layout of the two reference collector arrays with a gross collector area of 4800 m² each. The collector array using the harp collector is on the left, the meander array on the right. Overall size, row distance and piping configuration including some of the gradually reduced pipe diameters are shown.

distance and piping configuration including some of the gradually reduced pipe diameters are shown.

Both reference arrays presented in section 4.2 behave quite well in technical terms; see table 2 for a comprehensive overview of the results. The flow distribution is satisfactory without the need for using balancing valves. This results in good values for the 'stagnation distance' key figures: the minimum stagnation distance is quite high for both reference arrays (41.0 K for the harp, 41.5 K for the meander array) and is close to the average stagnation distance (44.4 K for both arrays). Consequently, the ratios of minimum to average stagnation distance are reasonably high (92.3% for the harp array, 93.6% for the meander array). This means that both collector arrays have low risk for partial stagnation.

Another evidence of the low partial stagnation risk becomes evident in the key figure 'efficiency loss due to uneven flow distribution': both collector arrays have very low values (0.03% for the harp, 0.04% for the meander array), meaning that the overall efficiency of the two reference collector arrays is barely affected by the degree of uneven temperature distribution.

A 'total flow inhomogeneity' or 'total flow skewness' may be defined as the ratio between maximum and minimum absorber mass flows, referring to all absorber pipes in the entire collector array. This measure has not been defined as a key figure in section 4.1 since it has no straightforward technical interpretation as opposed to the other key figures, which meet this requirement. The flow skewness factor, however, is well suited as a figure for relative comparison between the two reference arrays: The flow skewness value is 1.43 for the harp array and 1.75 for the meander array. These values are significantly higher than the threshold value of 1.22 proposed in [15], nevertheless both reference arrays show satisfactory technical behavior.

Table 1: Details of the reference collectors, the collector arrays and the assumed operating conditions

Reference collectors	
gross collector area	15.00 m²
aperture collector area	14.04 m²
efficiency values (η_0 / c_1 / c_2)	0.8 / 3.14 / 0.009
absolute thermal capacity (harp coll.)	128 kJ/K
absolute thermal capacity (meander coll.)	119 kJ/K

Reference collector arrays and operating conditions	
specific mass flow	16 kg/m²$_{abs}$·h
collector tilt angle	45°
supply (inflow) temperature	50°C
ambient temperature	20°C
global radiation in collector plane	1000 W/m²
heat transfer medium	propylene glycol
glycol concentration	40% v/v
absolute fluid pressure in collector	2.5 bar
boiling point of heat transfer fluid	130.6°C

Table 2: 'Classic' calculation results and results of the key figures defined in section 3.1.
The results are presented for both reference collector arrays defined in section 3.2.

'Classic' calculation results	harp collector array	meander collector array
Collector area: gross, aperture	4800 m²$_{gr}$, 4492 m²$_{ap}$	4800 m²$_{gr}$, 4492 m²$_{ap}$
Thermal power output: absolute, specific	2769 kW, 577 W/m²$_{gr}$	2763 kW, 576 W/m²$_{gr}$
Resulting flow temperature	86.3°C	86.2°C
Absorber temperatures (flow side): max, min	89.6°C, 84.2°C	89.0°C, 82.8°C
Overall thermal efficiency	62.2%	62.0%
Total flow skewness factor	1.43	1.75

Results of the key figures of section 4.1	harp collector array	meander collector array
Stagnation distance: minimum, average, min/avg.	41.0 K, 44.4 K, 92.3%	41.5 K, 44.4 K, 93.6%
Maximum flow velocity	1.69 m/s	1.71 m/s
Absorber pipe Reynolds numbers: min, max	3451, 8812	2839, 7169
Specific metal mass of array piping	0.84 kg$_{steel}$/m²$_{gr}$	0.50 kg$_{steel}$/m²$_{gr}$
Piping network length	~6.3 cm/m²$_{gr}$	~2.1 cm/m²$_{gr}$
Specific copper mass in solar collector	1.28 kg$_{Cu}$/m²$_{gr}$	1.96 kg$_{Cu}$/m²$_{gr}$
Thermal capacity of the collector array	11.3 kJ/m²$_{gr}$·K	9.6 kJ/m²$_{gr}$·K
Ratio of hydraulic to thermal power	1.37 W$_{hyd}$/kW$_{th}$	1.27 W$_{hyd}$/kW$_{th}$
Total pressure loss	1.94 bar	1.78 bar
Efficiency loss due to uneven flow distribution	0.03%	0.04%
Overall emptying behavior	bad	good

Although the total collector areas and the specific mass flows are identical for both reference collector arrays and the thermal performances are very similar, the Reynolds numbers in the absorber pipes do not match. This difference is a consequence of the chosen collector types and collector array designs. The minimum (maximum) absorber Re numbers are 3451 (8812) for the harp array and 2839 (7169) for the meander array. As explained in section 4.1, this results in higher collector efficiency due to improved heat transfer in the absorber pipe. The difference in Reynolds numbers is the main explanation for the slightly higher thermal power output, higher resulting flow temperature and higher overall thermal efficiency of the harp array compared to the meander array.

The maximum flow velocities in the collector arrays, however, are not in the absorber pipes, but in the connecting pipes. Both reference arrays reach high flow velocities (1.69 m/s for the harp, 1.71 m/s for the meander array), but these values might be acceptable – see also the statement in the definition of the key figure 'maximum flow velocity' in section 4.1.

The total pressure loss of the reference collector arrays is easy to handle (1.94 bar for the harp, 1.78 bar for the meander array) and do not cause any safety-related problems. These values are interesting if viewed together with the key figure 'ratio of hydraulic to thermal power', telling us that the harp array needs more pump electricity than the meander array in order to harvest the same solar thermal power. This is expressed by the number of 1.37 W_{hyd} of hydraulic power needed to get 1 kW_{th} thermal power for the harp array, while this number drops to 1.27 W_{hyd}/kW_{th} for the meander array, a reduction by 7%.

The two reference collectors have different internal piping dimensions (see figure 1). As a result, the specific copper mass of the meander collector is much higher (1.96 kg/m^2_{gr}) than in the harp collector (1.28 kg/m^2_{gr}), resulting in additional cost in terms of a more expensive collector, at least for what concerns the material cost. On the other hand, the hydraulic layout of the meander collector array allows shorter pipe lengths for the connecting pipe work, as the main supply pipe of the harp array (approx. 100 m long, see figure 2) is not necessary. In numbers, this fact becomes clear from the key figure 'specific metal mass of array piping', with a value of 0.84 kg_{steel}/m^2_{gr} for the harp array, but only 0.50 kg_{steel}/m^2_{gr} for the meander array.

Another difference between the piping of the two reference collector arrays is the piping network: For the harp array, the supply and return connecting pipes are on opposite sides, and one long supply pipe is needed, even if the array is connected in U, not in Z, shape (see figure 2). This results in a high value for the key figure 'piping network length' (6.3 cm/m^2_{gr}). The meander array not only gets rid of the main supply pipe, it also allows one central pipe channel bearing both the supply and the return pipes, so possibly only one trench needs to be excavated. This results in a much smaller piping network length (2.1 cm/m^2_{gr}).

Finally, a look at the thermal capacities of the two reference collector arrays reveals that both are thermally quite heavy. The reference collectors defined within the scope of this paper have absolute thermal capacities of 128 kJ/K (harp collector) and 119 kJ/K (meander collector). Together with the heavier piping for the harp array, the key figure 'thermal capacity of the collector array' is as high as 11.3 $kJ/m^2_{gr}\cdot K$ for the harp array, while for the meander array it sums up to 9.6 $kJ/m^2_{gr}\cdot K$, including all collector array piping. The meaning of these values becomes clear from a brief example calculation: Let us assume that the collector arrays need be heated up by 65 K in order to reach the average operation temperature; the capacitive energy losses then come to 0.20 kWh/m^2_{gr} for the harp array and 0.17 kWh/m^2_{gr} for the meander array. If we suppose a maximum specific daily energy yield of 3.3 kWh/m^2_{gr}, then the absolute capacitive energy losses would eat up as much as 6.2% (harp array) and 5.2% (meander array) of the energy yield. It becomes clear from this example that thermally lighter-weight collectors have the strong advantage of lower capacitive energy losses.

In case the authority of the collector rows compared to the connecting pipes is not high enough, flow distribution will deteriorate, leading to the detrimental effects described in section 4.1. If the row authority is not increased (for instance, by using larger pipe diameters for the connecting pipes), another option is to use balancing valves. To our opinion, however, the use of balancing valves should be avoided if stagnation cannot be excluded, as it is contradictory to the minimization of the levelized solar energy cost. Employing balancing valves and other accessories such as air bleeders in the collector array has several cost-relevant disadvantages: higher initial cost (additional investment), increased installation time (for the necessary mass flow balancing) and possibly high

ongoing costs (in case of defective valves). Following these considerations, the authors of this paper are in favor of achieving well-balanced flow distributions by appropriate choice of pipe diameters, as far as this is possible. Only in the case of very large collector arrays, using balancing valves is sometimes the only feasible solution – but it requires effective measures to protect against stagnation.

5. T-Pieces Pressure Loss Measurements

One important feature of solar collectors and collector arrays is the hydraulic performance in terms of pressure drop and flow distribution between parallel branches. Homogeneous flow distribution between absorber pipes is a key for both collector and collector arrays design – see section 4 for details.

5.1. Literature Research

The main technical unknown in hydraulic calculations are the T-pieces which are found in solar collectors, where small absorber pipes are connected with the larger header pipes. Surprisingly, although several comprehensive studies about the behavior of T-pieces are available – for instance, [6, 8, 14, 16] –, none of them covers the boundary conditions typically found in solar thermal installations. The main differences are:

1) Data in the mentioned sources are valid for $\mathrm{Re} > 2 \cdot 10^5$, fully turbulent flow. Typical Reynolds numbers in solar thermal plants, however, are much lower.
2) There are considerable differences between the pressure loss values reported in the mentioned literature sources, but a proper explanation of the deviations is missing.
3) The pressure loss values are only valid for idealized T-piece geometries: either sharp or defined-radius junctions are assumed. Investigations [9] have shown that, due to the employed manufacturing processes of solar collectors, T-pieces often have absorber pipes protruding into the header pipes (non-idealized geometry).

The contributions of Weitbrecht [18] and Badar [2] are relevant to solar collectors. Weitbrecht does provide results of experimental measurements, these, however, are limited to the laminar regime and assume an idealized geometry, with no change in depth of penetration. Badar, in his PhD thesis, deals with Reynolds numbers typical for solar thermal collectors, as well as absorber pipes that protrude into the collector pipes. His work contains no experimental results, but focuses on CFD simulations alone. Since the CFD model uncertainty is very difficult to handle in the transient region between laminar and turbulent flow (typical for solar thermal systems), a validation with experimental data is indispensable.

5.2. Experimental results

As shown above, previous research has failed to provide sufficient insight into the pressure loss behavior of T-pieces under conditions that are relevant for solar thermal collectors. In response, we have conducted a series of experiments in our own laboratory in order to find out these pressure loss values. The experiments aim at gaining detailed new insight into the minor pressure loss of T-pieces under boundary conditions typically found in solar thermal installations. While a description of the experimental setup is beyond the scope of this paper, we are going to present selected results. The experiments aim at determining the pressure loss coefficient ζ, based

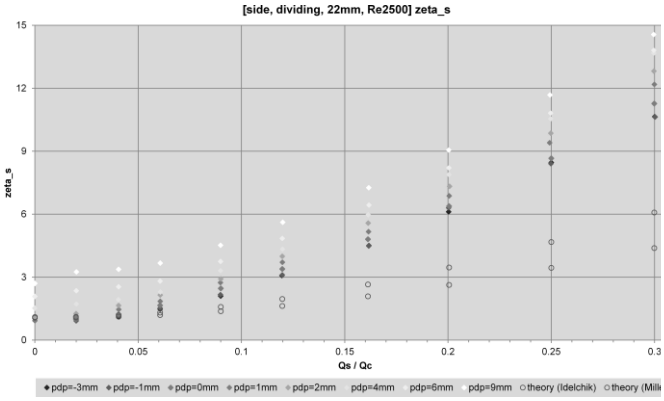

Figure 3: Characteristic curves of pressure loss coefficients ζ for dividing flow in a T-piece with a 22mm header pipe at Re=2500. The branching flow coefficients ζ_s are shown (greyish diamonds); lighter color means higher penetration depth. The empty circles are the results of two classic models (Idelchik, 2008) and (Miller, 2008).

on the minor pressure loss:

$$\Delta p_{minor} = \Delta p_{measured} - \Delta p_{friction} - \Delta p_{dynamic} \quad (1)$$

$$\zeta := \frac{\Delta p_{minor}}{\rho\, v_c^2/2} \quad (2)$$

We varied several influencing variables, covering a wide range of operating conditions of solar thermal systems:

1) Reynolds numbers range from deeply laminar flow (Re≈250) via the laminar-turbulent transition region up to fully turbulent flow (Re≈23,000).
2) real-world geometries, that is: absorber pipes protruding into the header pipes, a parameter which has been widely disregarded thus far. We attained varying penetration depths by employing a special, adjustable specimen able to reproduce penetration depths between +9mm and -3mm (equivalent to a perfectly rounded junction).
3) different area ratios (cross section ratio of absorber and header pipe). We examined 8x0.4mm absorber pipes in combination with header pipes of dimensions 42x1.5mm, 28x1mm, 22x0.8mm and 18x0.7mm
4) different volume flow ratios between side and common volume flows (see figures 3)

All measurements were performed under nearly isotherm conditions (fluid = ambient temperature) in order to minimize measurement error. Water was used as a test fluid. We examined both dividing and combining flow. Our measurement results show that – as expected – ζ values for T-pieces in solar collectors are generally higher than predicted by classical models (see figure 3). Another result is that in general, the penetration depth affects the ζ values.

The mathematical evaluation of the 5-dimensional characteristics of T-pieces data using a Neural Net technique and its full integration into the computational tool is ongoing work. In total, over 25,000 single measurements are available.

6. Conclusions

In the opinion of the authors, there are currently no satisfactory methods for a straightforward assessment and comparison of different design options for solar collector arrays. Based on accurate calculations of the relevant physical phenomena, we presented a framework of key figures that enable a novel approach to the engineering of large solar collector arrays. The key figures provide a basis for answering essential technical questions and they offer a way to characterize and assess different collector and collector array designs. However, the key figures also focus on the price of solar thermal energy as they take into account investment costs (e.g. effort for collector array piping), energy output (e.g. capacitive energy losses), ongoing costs (e.g. pump power) and safety issues (e.g. stagnation distance).

Moreover, we focused on T-pieces found in solar collectors where small absorber pipes are connected with the larger header pipes. The pressure losses of these T-pieces are largely unknown under the boundary conditions found in solar thermal systems. They are, however, important for calculating flow and temperature distribution and total pressure loss in solar collectors. Theoretical limits of collector and collector array design cannot be studied without detailed information about the technical behavior of T-pieces in terms of pressure losses. In response, we carried out an extensive experimental study measuring pressure loss values of T-pieces under boundary conditions which are typical of solar thermal systems. Our measurements generate information that cannot be found in standard scientific literature. This opens up new ways to simulate solar collectors and collector arrays in an accurate and technically reliable way. The mathematical modeling and evaluation of the measurements and the full integration into the computational tool [1] is ongoing work. Eventually, our results will allow drawing conclusions about allowable production tolerances and the influence of actual production technologies on the hydraulic behavior of solar collectors and collector arrays.

Altogether, we consider our work as a contribution to increased planning certainty and to lower-cost, high quality and trouble-free operation of large solar plants.

Acknowledgements

This project is supported by the Austrian Climate and Energy Fund and is carried out as part of the "Energy of the Future" program under contract number FFG 829854.

References

[1] AEE INTEC (1995-2013). Computational toolset for solar thermal collectors and collector arrays. AEE – Institute for Sustainable Technologies (AEE INTEC), Gleisdorf, Austria. (The tool is proprietary to AEE INTEC and not publicly available)

[2] Badar A.W., Buchholz R., Lou Y., Ziegler F., 2011. CFD Based Analysis of Flow Distribution in a Coaxial Vacuum Tube Solar Collector with Laminar Flow Conditions. Institut für Energietechnik, KT 2, FG Maschinen- und Energieanlagentechnik, Technische Universität Berlin.

[3] Bajura R.A. and Jones E.H., 1976. Flow Distribution Manifolds. Journal of Fluids Engineering, Vol. 98, No. 4, pp. 654-664.

[4] Dalenbäck J.-O., 2010. Success Factors in Solar District Heating. Deliverable 2.1 of the project 'SDHtake-off – Solar District Heating in Europe' (available in pdf format at www.solar-district-heating.eu).

[5] Duffie J.A. and Beckman W.A., 2006. Solar Engineering of Thermal Processes, 3rd edn. Wiley Interscience, New York.

[6] Idelchik I.E., 2008. Handbook of Hydraulic Resistance, 4th revised and augmented edn. Begell House Inc., Redding, USA.

[7] Jones G.F. and Lior N., 1994. Flow Distribution In Manifolded Solar Collectors With Negligible Buoyancy Effects. Solar Energy, Vol. 52, No. 3, pp. 289-300.

[8] Miller D.S., 2008. Internal Flow Systems, 2nd edn. Miller Innovations, Bedford, UK.

[9] Ohnewein Ph., Preiß D., Hausner R. and Fink Ch., 2012. Hydraulikdesign in solarthermischen Großanlagen. Proceedings of the OTTI symposium on thermal solar energy, 9-12 May, Bad Staffelstein, Germany.

[10] Peuser F.A., Croy R., Mies M., Rehrmann U. and Wirth H.P., 2009. Solarthermie-2000, Teilprogramm 2 und Solarthermie2000plus - Wissenschaftlich-technische Programmbegleitung und Messprogramm (Phase 3). ZfS – Rationelle Energietechnik GmbH, Hilden. (available at www.tu-chemnitz.de, in German only)

[11] Peuser F.A., Remmers K.-H. and Schnauss M., 2001. Langzeiterfahrung Solarthermie, Wegweiser für das erfolgreiche Planen und Bauen von Solaranlagen. Solarpraxis AG, Berlin. (in German)

[12] Remmers K.-H., 2001. Große Solaranlagen – Einstieg in Planung und Praxis. Solarpraxis AG, Berlin. (in German)

[13] SDH – Solar District Heating, 2012. Solar district heating guidelines. Deliverables 3.1 and 3.2 of the project 'SDHtake-off – Solar District Heating in Europe' (available in pdf format at www.solar-district-heating.eu).

[14] VDI – Verein Deutscher Ingenieure, 2006. VDI-Wärmeatlas, Zehnte, bearbeitete und erweiterte Auflage. Springer Verlag, Berlin Heidelberg. (in German)

[15] VDI – Verein Deutscher Ingenieure, 2004. VDI 6002 Solar heating for domestic water – General principles, system technology and use in residential building. Beuth Verlag, Berlin.

[16] Wagner W., 1997. Strömung und Druckverlust, 4. Auflage. Vogel Verlag, Würzburg. (in German)

[17] Wang X.A. and Wu L.G., 1990. Analysis and Performance of Flat-Plate Solar Collector Arrays. Solar Energy, Vol. 45, No. 2, pp. 71-78.

[18] Weitbrecht V., Lehmann D., Richter A., 2002. Flow Distribution in Solar Collectors with Laminar Flow Conditions. Solar Energy, Vol. 73, No. 6, 433-441.